***Regular Article***

# Mechanism-Based Pharmacokinetic–Pharmacodynamic Modeling of Luseogliflozin, a Sodium Glucose Co-transporter 2 Inhibitor, in Japanese Patients with Type 2 Diabetes Mellitus

Yoshishige Samukawa,[#] Masaru Mutoh,*[,#] Shi Chen, and Nobuo Mizui

*Taisho Pharmaceutical Co., Ltd.; 3–24–1 Takada, Toshima-ku, Tokyo 170–8633, Japan.*
Received December 20, 2016; accepted April 24, 2017

**Luseogliflozin is a selective sodium glucose co-transporter 2 (SGLT2) inhibitor that reduces hyperglycemia in type 2 diabetes mellitus (T2DM) by promoting urinary glucose excretion (UGE). A clinical pharmacology study conducted in Japanese patients with T2DM confirmed dose-dependency of UGE with once-daily administration of luseogliflozin; however, the reason for sustained UGE after plasma luseogliflozin decreased was unclear. To elucidate the effect of inhibition rate constants, $K_{on}$ and $K_{off}$, and to explain the sustained UGE, a pharmacokinetic–pharmacodynamic (PK-PD) model was built based on the mechanisms of glucose filtration in the glomerulus and reabsorption in the renal proximal tubule of kidney as well as the kinetics of competitive inhibition of SGLT1/2 and inhibition rate constants of SGLT2, by using UGE and plasma glucose levels and luseogliflozin concentrations. This acquired population PK-PD model adequately described the sustained UGE and the estimated population means of the inhibition constant for SGLT2 ($K_{i2}$) and inhibition-rate constants for SGLT2 ($K_{on}$ and $K_{off}$) were 0.31- and 3.6-fold lower or higher than the *in vitro* values. Because the dissociation half-time of luseogliflozin from SGLT2 calculated from $K_{off}$, 6.81 h, was consistent with the value *in vitro*, we considered that the sustained UGE could be explained by the long dissociation half-time. Moreover, by calculating the SGLT2 inhibition ratio using the model, we discuss other properties of the UGE time course after luseogliflozin administration.**

**Key words** luseogliflozin; urinary glucose excretion; pharmacokinetic–pharmacodynamic model; sodium glucose co-transporter 2; type 2 diabetes mellitus

In the human kidney, plasma glucose entering the glomeruli is filtered into the nephron fluid, and the filtered glucose is reabsorbed almost completely by two isoforms of sodium glucose co-transporter (SGLT), SGLT2 and SGLT1. SGLT2 is a high-capacity, low-affinity glucose transporter located in the early convoluted segment (S1 segment) of the proximal tubule that mediates 90% of renal glucose reabsorption. SGLT1 is a high-affinity, low-capacity glucose transporter located in the straight section of the proximal tubule (S3 segment) that is responsible for 10% of renal glucose reabsorption.[1)] Inhibition of SGLT2 causes glucose excretion in urine and a reduction in plasma glucose. Several SGLT2 inhibitors have been developed for treatment of type 2 diabetes mellitus (T2DM).[2–4)]

Luseogliflozin is a novel selective SGLT2 inhibitor[5,6)] currently marketed for the treatment of T2DM. The recommended dose is 2.5 mg (or 5 mg depending on the symptoms) once daily before or after breakfast. Studies in Japanese patients with T2DM have confirmed that treatment with luseogliflozin increases urinary glucose excretion (UGE) and reduces plasma glucose levels.[7–12)]

In a clinical pharmacology study conducted in Japanese patients with T2DM, reported by Sasaki *et al.*, intensive sampling of UGE (nine sampling intervals a day) was performed and UGE change from pre-dose was analyzed; a significant increase in UGE was observed with once-daily luseogliflozin administration. The UGE was dose-dependent and the relationship of change in daily UGE and area under the curve $(AUC)_{0-24h}$ of plasma luseogliflozin could be expressed by means of the $E_{max}$ model.[9)]

However, the time courses of UGE over 24 h after luseogliflozin administration have not sufficiently been explained. Sasaki *et al.* found that UGE was maintained after supper at the same degree as after breakfast and apparently conflicted with the time course of plasma luseogliflozin.[9)] Accordingly, we attempted to build the mechanism-based pharmacokinetic–pharmacodynamic (PK-PD) model to predict those features of the UGE time course.

Although previous studies have reported particular PK-PD models to evaluate the UGE of SGLT2 inhibitors,[13–19)] only four have adopted the mechanism-based PK-PD models: the PK-PD model for tofogliflozin in rats[16,17)] and the PK-PD model of dapagliflozin and canagliflozin in humans.[18,19)] In these studies, the investigators adopted the physiological construction of the proximal tubule in the kidney and the kinetics of competitive SGLT1/2 inhibition in their PK-PD model and successfully described the time course of UGE. As luseogliflozin was found to be a competitive inhibitor for SGLT2 through *in vitro* experiments in human SGLT2-expressing cells,[20,21)] we adopted the kinetics of competitive inhibition for SGLT1/2. Moreover, the rate constants for association of luseogliflozin to SGLT2 ($K_{on}$) and for dissociation of luseogliflozin from SGLT2 ($K_{off}$) have been reported in these studies. Because the dissociation half-time of luseogliflozin from SGLT2 calculated from $K_{off}$ was about 7.0 h, we assumed that sustained UGE after supper with luseogliflozin administration depends on the long dissociation half-time. We then considered those rate constants for PK-PD modeling of luseogliflozin.

In the present study, we constructed a mechanism-based PK-PD model that can describe the dose-dependency and time

[#] These authors contributed equally to this work.

* To whom correspondence should be addressed. e-mail: m-mutou@so.taisho.co.jp

course of sustained UGE after luseogliflozin administration. We used a known physiological construction of the proximal tubule and the relative locations of SGLT1/2 in the proximal tubule, and considered the kinetics of competitive inhibition of SGLT1/2 and inhibition rate constants of SGLT2. Our purpose was to elucidate the mechanism of UGE with luseogliflozin and to confirm the effect of inhibition rate constants on UGE by administration of luseogliflozin.

## METHODS

**Chemicals** Luseogliflozin, (2*S*,3*R*,4*R*,5*S*,6*R*)-2-{5-[(4-ethoxyphenyl)methyl]-2-methoxy-4-methylphenyl}-6-(hydroxymethyl)-thiane-3,4,5-triol hydrate; $C_{23}H_{30}O_6S\ xH_2O$; molecular weight (for anhydrate) 434.55 (Fig. 1).

**Study Design, Population, and PK and PD Data** PK and PD data were acquired from four active groups of the clinical pharmacology study performed in Japanese outpatients with T2DM whose glycated hemoglobin (HbA1c) ranged from 6.9 to 10.3%.[9] Thirty-one patients (26 male and 5 female) were allocated to four luseogliflozin dose groups: 0.5 mg ($n$=7), 1 mg ($n$=8), 2.5 mg ($n$=8), and 5 mg ($n$=8), once daily before breakfast for 7 d. They were prescribed a stable therapeutic diet, and oral antidiabetic drugs and insulin were prohibited for 4 weeks before administration of the study drug. Only two patients had taken oral antidiabetic drugs 4 weeks before study drug administration. Age, weight, body mass index, estimated glomerular filtration rate (eGFR),[22] fasting plasma glucose (FPG), and UGE at baseline (before first luseogliflozin administration) of patients ranged from 43 to 74 years, 51.9 to 99.3 kg, 19.1 to 32.0 kg/m$^2$, 59 to 116 mL/min, 113 to 229 mg/dL, and 0.3 to 81.4 g/d, respectively (Table 1). Patients consumed a standardized meal of approximately 600 kcal (approximately 16% protein, 21% fat, and 63% carbohydrate) just after luseogliflozin administration (0 h), and 4 and 12 h later on days 1 and 7. On day −1, they consumed this standardized meal at the same time points as on days 1 and 7.

Plasma concentrations of luseogliflozin were measured at 0, 0.25, 0.5, 1, 1.5, 2, 3, 4, 6, 8, 12, and 24 h after luseogliflozin administration on days 1 and 7 and at 48, 72, and 96 h after luseogliflozin administration on day 7 (Supplementary Fig. S1). In addition, plasma glucose levels were measured at 0, 0.5, 1, 2, 4, 4.5, 5, 6, 8, 12, 12.5, 13, 14, 16, and 24 h after the start of breakfast on day −1; at 0, 0.5, 1, 2, 4, 4.5, 5, 6, 8, 12, 12.5, 13, 14, 16, and 24 h after luseogliflozin administration on days 1 and 7; and at 96 h after luseogliflozin administration on day 7 (Supplementary Fig. S1). Urinary glucose samples were collected at 0–2, 2–4, 4–6, 6–8, 8–10, 10–12, 12–14, 14–16, and 16–24 h after the start of breakfast on day −1; at 0–2, 2–4, 4–6, 6–8, 8–10, 10–12, 12–14, 14–16, and 16–24 h after luseogliflozin administration on days 1 and 7; and at 24–48, 48–72, and 72–96 h after luseogliflozin administration on day

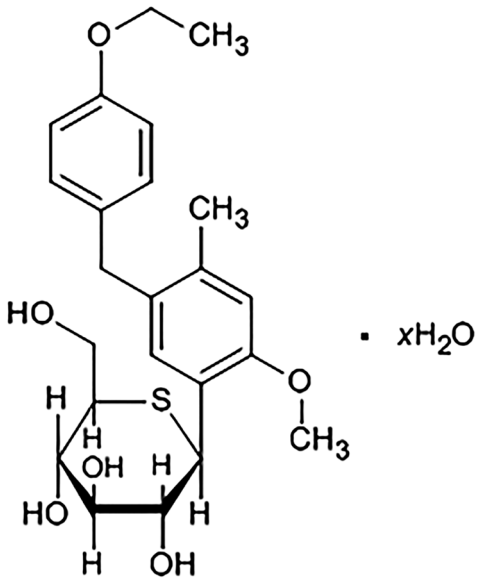


Fig. 1. Structural Formula of Luseogliflozin

Table 1. Patient Characteristics at Baseline

| | | Dose | | | | Total |
|---|---|---|---|---|---|---|
| | | 0.5 mg | 1 mg | 2.5 mg | 5 mg | |
| Number of subjects | | 7 | 8 | 8 | 8 | 31 |
| Gender | (male/female) | 6/1 | 6/2 | 8/0 | 6/2 | 26/5 |
| Age | (years) | 57.1±9.7 (46–71) | 59.8±10.8 (43–74) | 55.9±8.8 (45–68) | 57.6±8.2 (47–69) | 57.6±9.0 (43–74) |
| Weight | (kg) | 67.71±14.40 (51.9–92.9) | 72.12±18.57 (52.4–99.3) | 68.00±7.90 (58.6–76.6) | 71.80±9.59 (57.5–82.3) | 69.98±12.74 (51.9–99.3) |
| BMI | (kg/m$^2$) | 23.55±3.62 (20.8–30.1) | 25.94±4.98 (19.1–32.0) | 24.38±3.35 (19.9–29.2) | 26.13±2.83 (21.3–29.1) | 25.05±3.75 (19.1–32.0) |
| eGFR | (mL/min) | 88.6±16.9 (61–110) | 90.8±16.9 (71–113) | 90.5±13.7 (62–106) | 92.5±25.2 (59–116) | 90.6±17.8 (59–116) |
| HbA1c | (%) | 8.26±1.05 (7.4–10.3) | 7.61±1.01 (6.9–9.4) | 8.30±1.08 (7.3–10.2) | 7.59±1.01 (7.0–10.3) | 8.33±1.04 (6.9–10.3) |
| FPG | (mg/dL) | 166.0±29.1 (142–209) | 151.3±32.0 (113–201) | 166.5±37.9 (122–229) | 150.1±22.0 (122–183) | 158.2±30.3 (113–229) |
| UGE | (g/d) | 33.5±25.0 (0.466–79.1) | 17.0±15.3 (1.10–42.6) | 44.1±29.4 (7.79–81.4) | 16.2±14.0 (0.329–45.7) | 27.5±23.9 (0.329–81.4) |

Displayed by the mean±S.D. (min–max) except gender and number of subjects. BMI, body mass index; eGFR, estimated glomerular filtration rate; HbA1c, haemoglobin A1c; FPG, fasting plasma glucose; UGE, urinary glucose excretion.

7. Measurements of plasma concentration of luseogliflozin, plasma glucose level, and urinary glucose have been described previously.[7)]

**Ethical Approval** We analyzed PK and PD data from Japanese patients with T2DM enrolled in a clinical pharmacology study, which was conducted in accordance with the ethical standards of the Helsinki Declaration and the Japanese Pharmaceutical Affairs Law and Good Clinical Practice. The study protocol was approved by the Institutional Review Board of P-One Clinic, Keikokai Medical Corporation. The study design, study population, and PK and PD data outlined here are the only data analyzed in this report. Additional information is provided in a previous report.[9)]

**Informed Consent** Informed consent was obtained from all individual participants included in the clinical study.

**PD Model Structure** A PD model was developed based on the mechanisms of luminal glucose reabsorption by SGLT1/2 for analysis of UGE at day −1 to estimate individual $V_{max2}$ and $V_{max1}$. Glucose reabsorption rate without an inhibitor is simply described by the Michaelis–Menten process as Eq. (1):

$$v = V_{max,j} \times Glu / \{K_{m,j} + Glu\} \quad (1)$$

where v is the glucose reabsorption rate of SGLTs, $V_{max,j}$ is the transport capacity of SGLT1 ($j$=1) and SGLT2 ($j$=2), Glu is the luminal glucose, and $K_{m,j}$ is the glucose affinity for SGLT1 ($j$=1) and SGLT2 ($j$=2). Moreover, we used the rate constant "$K_g$" to describe the time lag of excretion derived in the tubule. UGE rate at 2–4 h after each meal was higher than that at 0–2 h (Table 2). On the other hand, the *AUC* of plasma glucose 2–4 h was lower than at 0–2 h (Table 2). Because the UGE peak was delayed after the *AUC* peak of plasma glucose, we assumed a lag time after the proximal tubule and before urine excretion to fit the observed UGE (Fig. 2). The lag was also observed in the absence of luseogliflozin at day −1 (Table 2); therefore, we set the $K_g$ in the PD model. In the PD model, the Michaelis–Menten process and rate constant $K_g$ were adopted for the population analysis of UGE at day −1 to estimate the individual $V_{max2}$ and $V_{max1}$.

**PK-PD Model Structure** In the presence of luseogliflozin, glucose reabsorption by SGLT1/2 is inhibited by luseogliflozin, and glucose is excreted in urine. Luseogliflozin is a competitive inhibitor of SGLT2.[20)] Because luseogliflozin competes with glucose for SGLT1/2 within renal tubule segments 1 and 3, it was also thought to be a competitive, rather than an uncompetitive or noncompetitive, inhibitor to SGLT1. As the inhibition is competitive, the glucose reabsorption rate of SGLT1/2 inhibited by luseogliflozin is represented by Eq. (2).[23)]

$$v = V_{max,j} \times Glu / \{K_{m,j} \times (1 + Luseo / K_{i,j}) + Glu\} \quad (2)$$

where $v$ is the glucose reabsorption rate of SGLTs, $V_{max,j}$ is the transport capacity of SGLT1 ($j$=1) and SGLT2 ($j$=2), Glu is the luminal glucose, $K_{m,j}$ is the glucose affinity for SGLT1 ($j$=1) and SGLT2 ($j$=2), Luseo is the luminal luseogliflozin

Table 2. UGE Rate and Partial *AUC* of Plasma Glucose of Each Meal on Days −1 and 7

| Variables | Time interval (after administration) | Unit | Dose | | | |
|---|---|---|---|---|---|---|
| | | | 0.5 mg | 1 mg | 2.5 mg | 5 mg |
| Day 7 | | | | | | |
| UGE rate | After breakfast (0–2 h) | (g/h) | 4.0 (1.5) | 4.9 (1.3) | 7.0 (3.0) | 6.9 (1.5) |
| | After breakfast (2–4 h) | (g/h) | 4.4 (1.5) | 5.2 (1.5) | 6.9 (1.8) | 6.1 (2.1) |
| | After lunch (4–6 h) | (g/h) | 4.5 (1.4) | 4.7 (1.6) | 6.8 (1.6) | 6.0 (1.9) |
| | After lunch (6–8 h) | (g/h) | 6.6 (2.6) | 6.2 (1.8) | 8.6 (2.7) | 7.9 (3.2) |
| | After supper (12–14 h) | (g/h) | 3.0 (1.0) | 3.3 (0.9) | 5.3 (0.7) | 4.8 (1.2) |
| | After supper (14–16 h) | (g/h) | 5.5 (2.2) | 4.2 (1.3) | 7.4 (1.5) | 7.3 (1.8) |
| Partial *AUC* of plasma glucose | After breakfast (0–2 h) | (mg·h/dL) | 427 (65) | 422 (65) | 389 (52) | 384 (40) |
| | After breakfast (2–4 h) | (mg·h/dL) | 383 (93) | 359 (57) | 349 (54) | 325 (51) |
| | After lunch (4–6 h) | (mg·h/dL) | 409 (91) | 372 (57) | 376 (59) | 338 (44) |
| | After lunch (6–8 h) | (mg·h/dL) | 477 (119) | 414 (73) | 426 (71) | 372 (63) |
| | After supper (12–14 h) | (mg·h/dL) | 413 (34) | 377 (58) | 374 (31) | 348 (63) |
| | After supper (14–16 h) | (mg·h/dL) | 511 (75) | 448 (74) | 454 (34) | 407 (78) |
| Day −1 | | | | | | |
| UGE rate | After breakfast (0–2 h) | (g/h) | 1.4 (1.3) | 1.3 (1.1) | 2.2 (1.5) | 1.3 (0.7) |
| | After breakfast (2–4 h) | (g/h) | 2.0 (1.4) | 1.1 (1.1) | 2.8 (2.3) | 1.6 (1.7) |
| | After lunch (4–6 h) | (g/h) | 2.3 (1.7) | 0.7 (0.6) | 2.8 (1.9) | 1.0 (1.0) |
| | After lunch (6–8 h) | (g/h) | 2.7 (2.3) | 0.8 (0.6) | 3.7 (2.7) | 1.2 (2.0) |
| | After supper (12–14 h) | (g/h) | 1.4 (0.9) | 0.6 (0.5) | 1.6 (1.3) | 0.6 (0.5) |
| | After supper (14–16 h) | (g/h) | 3.2 (2.0) | 1.9 (1.7) | 3.6 (2.2) | 1.3 (1.1) |
| Partial *AUC* of plasma glucose | After breakfast (0–2 h) | (mg·h/dL) | 481 (75) | 472 (79) | 521 (93) | 461 (48) |
| | After breakfast (2–4 h) | (mg·h/dL) | 469 (110) | 414 (89) | 497 (116) | 415 (66) |
| | After lunch (4–6 h) | (mg·h/dL) | 529 (94) | 440 (70) | 528 (95) | 418 (62) |
| | After lunch (6–8 h) | (mg·h/dL) | 534 (114) | 435 (91) | 535 (107) | 411 (60) |
| | After supper (12–14 h) | (mg·h/dL) | 489 (64) | 437 (60) | 489 (103) | 414 (63) |
| | After supper (14–16 h) | (mg·h/dL) | 545 (102) | 507 (95) | 560 (89) | 468 (67) |

Values are mean (S.D.). *AUC*, area under the curve; UGE, urinary glucose excretion.

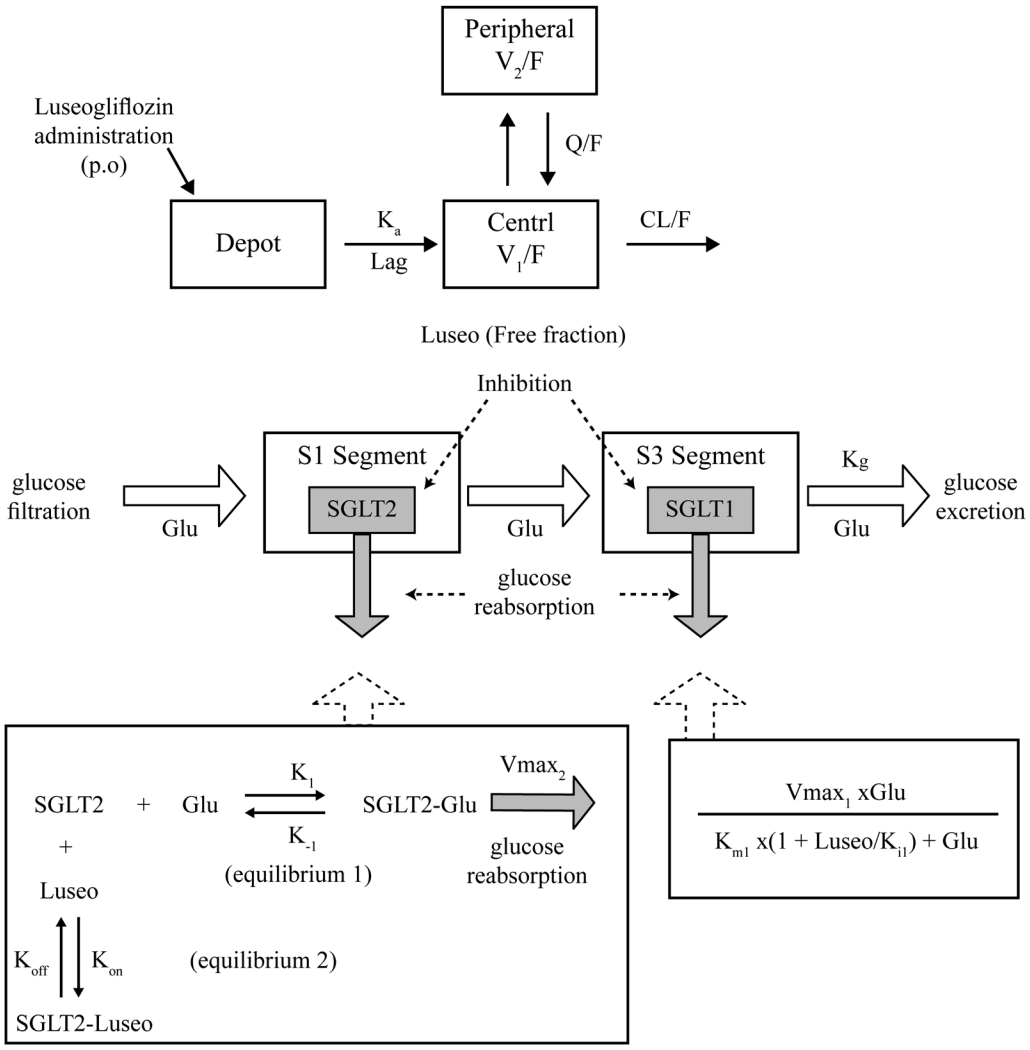


Fig. 2. Pharmacokinetic–Pharmacodynamic Model of Urinary Glucose Excretion, Model 2

$K_a$, absorption rate constant; Lag, absorption lag time; $V_1/F$, volume of distribution of central compartment; $V_2/F$, volume of distribution of peripheral compartment, CL/F, oral clearance; Q/F, inter-compartmental clearance; Glu, luminal glucose; Luseo, luminal luseogliflozin=free fraction of luseogliflozin; $K_1$, $K_{-1}$ rate constants of equilibrium 1; $K_{on}$, inhibition on rate of equilibrium 2; $K_{off}$, inhibition off rate of equilibrium 2; $K_g$, rate constant for excretion lag time; SGLT2, sodium glucose co-transporter 2; SGLT2-Glu, SGLT2-glucose complex; SGLT2-Luseo, SGLT2-luseogliflozin complex; $V_{max1}$, transport capacity of SGLT1; $V_{max2}$, transport capacity of SGLT2; $K_{m1}$, glucose affinity for SGLT1.

concentration, and $K_{i,j}$ is the inhibition constant of luseogliflozin to SGLT1 ($j$=1) and SGLT2 ($j$=2). Equation (2) was used in "PK-PD model 1" to calculate the reabsorption rate of SGLT1/2.

However, as the inhibition rate constant of luseogliflozin for SGLT2 was small, the glucose reabsorption rate could not be simply expressed by Eq. (2). Regarding the kinetics of inhibition rate constants, Dahl reported that smaller $K_{on}$ and $K_{off}$ values led to slowing of the association and dissociation reactions.[24] Hummel *et al.* reported that the inhibition rate constant $K_{on}$ of phlorizin, an SGLT2 inhibitor, was 9.72 1/nM/h and $K_{off}$ was 108 1/h,[25] which were large values, and the dissociation half-time ($T_{1/2,off}$) was 24 s, which was very small. Compared with phlorizin, the $K_{on}$ and $K_{off}$ of luseogliflozin for SGLT2 (0.084 1/nM/h and 0.11 1/h, respectively) were small and the $T_{1/2,off}$ (7.0 h) was large.[20] Accordingly, the reabsorption rate of SGLT2 inhibited by luseogliflozin should be expressed as a product of $V_{max2}$ and fraction of SGLT2-Glu complex (Eq. 3). The fraction of SGLT2-Glu complex is calculated using three differential Eqs. (4)–(6) in consideration of $K_{on}$ and $K_{off}$.[26]

$$v = V_{max2} \times [\text{SGLT2-Glu}] \tag{3}$$

$$\begin{aligned} &d[\text{SGLT2}]/dt \\ &= -(K_1 \times \text{Glu} + K_{on} \times \text{Luseo}) \\ &\quad \times [\text{SGLT2}] + K_{-1} \times [\text{SGLT2-Glu}] + K_{off} \\ &\quad \times [\text{SGLT2-Luseo}] \end{aligned} \tag{4}$$

$$\begin{aligned} &d[\text{SGLT2-Luseo}]/dt \\ &= -K_{off} \times [\text{SGLT2-Luseo}] + K_{on} \times [\text{SGLT2}] \times \text{Luseo} \end{aligned} \tag{5}$$

$$\begin{aligned} &d[\text{SGLT2-Glu}]/dt \\ &= -K_{-1} \times [\text{SGLT2-Glu}] + K_1 \times [\text{SGLT2}] \times \text{Glu} \end{aligned} \tag{6}$$

where $v$ is the glucose reabsorption rate of SGLT2 inhibited by Luseo, $V_{max2}$ is the transport capacity of SGLT2, [SGLT2-Glu] is the fraction of SGLT2-glucose complex, [SGLT2] is the fraction of free SGLT2, [SGLT2-Luseo] is the frac-

tion of SGLT2-luseogliflozin complex, [SGLT2]+[SGLT2-Glu]+[SGLT2-Luseo]=1, $K_1$ and $K_{-1}$ are rate constants, $K_{-1}/K_1=K_{m2}$ (equilibrium 1 in Fig. 2), and $K_{m2}$ is the glucose affinity for SGLT2. In "PK-PD model 2," the reabsorption rates of SGLT1 and SGLT2 were calculated by Eqs. 2 and 3, respectively.

In order to verify the need for $K_{on}$ and $K_{off}$, both PK-PD models 1 and 2 were compared. For this mechanism-based PK-PD model, several assumptions were adopted. The free fraction of luseogliflozin calculated from a plasma protein binding of 96%[27] was assumed to be the same as the luminal luseogliflozin concentration in the proximal tubule. The glucose level just after filtration in the glomerulus was assumed to be consistent with the plasma glucose level and then was devoted to reabsorption. eGFR was used for the flow rate of glucose until segment 3 in the proximal tubule.

**PK Model Analysis** The plasma luseogliflozin concentrations of 31 patients with T2DM were individually analyzed using a 2-compartment model with first-order absorption and absorption lag time. Basic statistics of PK parameters were calculated.

**PK-PD Model Analysis** For the PK-PD analysis, we used the time course of individual plasma glucose levels and the free fraction of plasma luseogliflozin concentration and performed a nonlinear mixed effect model analysis to predict the UGE of each collection interval to estimate parameters. For accurate PK-PD regression, we used predicted plasma luseogliflozin concentrations calculated from individually estimated PK parameters analyzed by WinNonlin using a 2-compartment model with first-order absorption and absorption lag time. Subsequently, these concentrations were converted to free fractions and used for PK-PD modeling. If there was a time point at which plasma glucose level was absent for regression of UGE, values of this time point were linearly interpolated using observed values.

Although $V_{max1}$ and $V_{max2}$ were fundamental to predicting UGE, we found no literature regarding the *in vitro* estimation of $V_{max}$. Accordingly, we estimated individual $V_{max1}$ and $V_{max2}$ by population analysis using data from day −1, the day before luseogliflozin administration. The model-building process reported here was performed by following two steps:

1. Population analysis of UGE at day −1 using PD model and estimation of individual $V_{max1}$ and $V_{max2}$

2. Population analysis of UGE after luseogliflozin administration using PK-PD model and estimation of PK-PD parameters

Step 1: Population Analysis of UGE at Day −1 Using PD Model and Estimation of Individual $V_{max1}$ and $V_{max2}$

Population analysis of UGE from 31 patients with T2DM at day −1 was performed using a PD model with $K_{m1}$ and $K_{m2}$ fixed to *in vitro* estimated values, 1.8 and 4.9 mM, respectively.[28] Normal distribution was assumed for intra-individual variability. Log-normal distribution was assumed for inter-individual variability of PD parameters, $V_{max1}$, $V_{max2}$, and $K_g$. Individual $V_{max1}$ and $V_{max2}$ values were estimated by the POSTHOC option. A PD model with rate constant $K_g$ was compared to a PD model without $K_g$ based on the deterioration of objective function (OBJ) and visual inspection of the scatter plot of observed UGE against individually predicted UGE in both models. Residual plots against time in both models were made to confirm the necessity of $K_g$. Basic statistics of estimated $V_{max1}$, $V_{max2}$, and contribution of $V_{max}$ {$V_{max1}/(V_{max1}+V_{max2})$} were calculated. Moreover, exploratory analyses of correlation between $V_{max}$ and background data were performed. Age, body weight, body mass index, eGFR, total bilirubin, HbA1c, FPG, and albumin were analyzed by regression analysis to $V_{max}$, and significant variables were analyzed as covariates by NONMEM based on the OBJ using the log-likelihood ratio test. A $p$ value of 0.05, representing a decrease in the OBJ of 3.84, was considered statistically significant (chi square distribution, degrees of freedom=1).

Step 2: Population Analysis of UGE after Luseogliflozin Administration Using PK-PD Model and Estimation of PK-PD Parameters

Population mean and inter-individual variability of PK-PD parameters, $K_{i2}$ (and $K_{on}$ for model 2) were estimated using nonlinear mixed-effects modeling based on the two PK-PD models. Normal distribution was assumed for intra-individual variability. Log-normal distribution was assumed for inter-individual variability of PK-PD parameters, $K_{i2}$ (and $K_{on}$ for model 2). In this analysis, $K_{m1}$ and $K_{m2}$ values from the literature[28] and individually estimated $V_{max1}$ and $V_{max2}$ in step 1 were used as fixed values. For model 2, $K_{off}$ was calculated using $K_{i2}$ and $K_{on}$ ($K_{off}=K_{i2}\times K_{on}$).[25] $T_{1/2,off}$ was calculated by $\log_e 2/K_{off}$.[28] Comparison between both models was based on the deterioration of OBJ and visual inspection of the scatter plot of observed UGE against the individually predicted UGE of both models. Moreover, the observed UGE and individually predicted mean was plotted against time after administration for evaluation of fitting to characteristic time course of UGE caused by luseogliflozin.

Sensitivity Analysis of $K_{i1}$ and $K_1$

We found no literature regarding the $K_{i1}$ of luseogliflozin and $K_1$ for SGLT2. We estimated $K_{i1}$ using *in vitro* selectivity of luseogliflozin of 1770, which was the $IC_{50}$ of SGLT1 divided by $IC_{50}$ of SGLT2.[5] The estimated $K_{i1}$ value was 1950 nM (1770-fold the $K_{i2}$ value of 1.10 nM). To confirm the validity of the $K_{i1}$ value, a sensitivity analysis using $K_{i1}$ values of 195, 1950, and 19500 nM was performed using a selected population PK-PD model. There was also no literature regarding $K_1$ value for SGLT2-Glu complex in equilibrium 1 (Fig. 2). If rapid equilibrium is assumed, $K_1$ must be large enough not to generate a binding delay between SGLT2 and glucose.[29] All NONMEM analyses were done with a $K_1$ value of 10. Sensitivity analysis using $K_1$ values of 0.3, 1, and 3 1/(mg/dL)/h was performed using a selected population PK-PD model.

Time Course of Inhibition Ratio of SGLT2

To speculate on the reason for the characteristic time course of UGE caused by luseogliflozin, the mean predicted inhibition ratios of SGLT2 against time on day 7 in PK-PD models 1 and 2 were plotted for each dose. The predicted inhibition ratio of SGLT2 was calculated as a fraction of the SGLT2-luseogliflozin complex in PK-PD model 2. The predicted inhibition ratio of SGLT2 in PK-PD model 1 was calculated by Eq. (2).

**PK-PD Model Validation** The population PK-PD model selected from the goodness-of-fit plots was evaluated using a nonparametric visual predictive check. Simulation datasets of 1000 subjects per dose were produced. Recommended doses of 2.5 and 5 mg were selected. Dosage, plasma glucose data, and individually estimated $V_{max1}$ and $V_{max2}$ values were repeatedly sampled from the population PK-PD modeling

dataset. PK parameters for 1000 subjects by dose were randomly simulated from basic statistics of each PK parameter. Plasma luseogliflozin concentration was calculated using these PK parameters and then using the converted free fraction of luseogliflozin. UGE was simulated based on the selected population PK-PD model in which the population mean and inter-individual variability of $K_{i2}$ (and $K_{on}$ for model 2), as well as the intra-individual variability, were fixed. A 5, 50, and 95th percentile of predicted UGE was created for each time point, and the prediction was evaluated by visual inspection.[30]

**Software** Compartment model analysis of plasma concentrations of luseogliflozin was performed using Phoenix WinNonlin (version 6.2, Certara). UGE regression analysis and simulation were performed using NONMEM (version 7.2, ICON). The first-order conditional estimation (FOCE) method was selected for the estimation algorithm. SAS (version 9.2, SAS Institute Inc.) was used to calculate basic statistical values and to prepare datasets for NONMEM and for Phoenix WinNonlin.

## RESULTS

**PK Model Analysis** Plasma luseogliflozin concentrations of 31 patients with T2DM were individually analyzed. The geometric mean and coefficient of variation of PK parameters (oral clearance, volume of distribution of central compartment, volume of distribution of peripheral compartment, inter-compartmental clearance, absorption rate constant, and absorption lag time) were 2.78 L/h (14.9%), 21.1 L (25.7%), 18.9 L (35.1%), 3.69 L/h (75.4%), 20.3 1/h (49.2%), and 0.174 h (40.7%), respectively.

**PK-PD Model Analysis**

Step 1: Population Analysis of UGE at Day −1 Using PD Model and Estimation of Individual $V_{max1}$ and $V_{max2}$

The population PD parameter was estimated by PD analyses of both models. NONMEM regressions were successfully converged in both models with $K_g$ and without $K_g$. Population parameters are presented in Table 3. The OBJ of PD model with $K_g$ decreased by 250.979 compared with the model without $K_g$ and residual (intra-individual) error also decreased from 2.18 to 1.28. Scatter plots of observed UGE against individually predicted UGE in both models are shown in Fig. 3. Residual plots against time in both models are shown in Fig. 4. These plots indicated that introducing $K_g$ to the PD model improved prediction accuracy and diminished the prediction bias by time interval. The mean $V_{max1}$ was 30 g/d and ranged from 14 to 53 g/d. The mean $V_{max2}$ was 376 g/d and ranged from 228 to 465 g/d. The mean contribution of $V_{max1}\{V_{max1}/(V_{max2}+V_{max1})\}$ was 7% and ranged from 3 to 11%. eGFR was significantly related with $V_{max1}$ and $V_{max2}$, $p=0.047$ and $p<0.001$, respectively (Fig. 5). However, eGFR was not covariate for $V_{max1}$ and $V_{max2}$ in the population analysis by NONMEM.

Step 2: Population Analysis of UGE after Luseogliflozin Administration Using PK-PD Model and Estimation of PK-PD Parameters

The population PK-PD parameters were estimated by PK-PD analyses of both models. NONMEM regressions were successfully converged for all analyses. PK-PD parameters and comparison with parameters *in vitro* are presented in Table 4. The population mean of $K_{i2}$ was estimated as 0.251 nM in model 1. On the other hand, the population means of $K_{i2}$ and $K_{on}$ were estimated as 0.336 nM and 0.303 1/nM/h, respectively,

Table 3. Population Analysis of Pharmacodynamic Models

| PD model | Parameter estimate | | | | | | | |
|---|---|---|---|---|---|---|---|---|
| | $V_{max2}$ g/d | $V_{max1}$ g/d | $K_g$ 1/h | $\omega V_{max2}$ — | $\omega V_{max1}$ — | $\omega K_g$ — | Residual g | OBJ |
| Model without $K_g$ | 360 | 56.6 | — | 0.159 | 0.345 | — | 2.18 | 775.785 |
| Model with $K_g$ | 374 | 31.9 | 1.19 | 0.171 | 0.863 | 0.133 | 1.28 | 524.806 |

PD, pharmacodynamic; $V_{max1}$, transport capacity of SGLT1; $V_{max2}$, transport capacity of SGLT2; $K_g$, rate constant for excretion lag time; $\omega V_{max2}$, interindividual variability of $V_{max2}$; $\omega V_{max1}$, interindividual variability of $V_{max1}$; $\omega K_g$, interindividual variability of $K_g$; OBJ, objective function of NONMEM; SGLT, sodium glucose co-transporter.

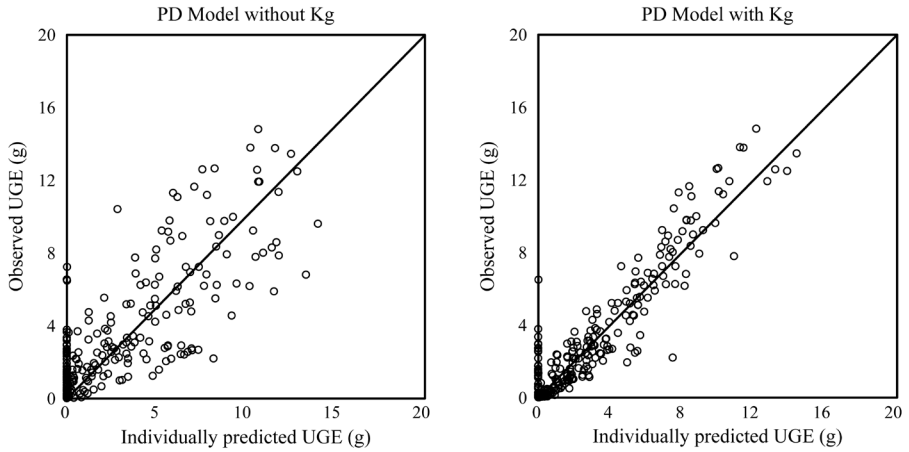


Fig. 3. Goodness-of-Fit Plots of Pharmacodynamic Models, with $K_g$ and without $K_g$

Line, observed UGE=individually predicted UGE; Open circles, plot of individual UGE; $K_g$, rate constant for excretion lag time; PD, pharmacodynamic; UGE, urinary glucose excretion.

in model 2. $K_{off}$ and $T_{1/2,off}$ were calculated as 0.102 1/h and 6.81 h, respectively. The addition of $K_{on}$ to model 2 reduced residual (intra-individual) error from 5.43 to 4.71 and improved the fit (⊿OBJ=−176.441). Scatter plots of observed UGE against individually predicted UGE in both models are shown in Fig. 6. Individual points in model 2 assembled to solid line compared with model 1. This indicated that model 2 improved prediction. Plots of observed UGE and individually predicted mean against time after administration are shown in Fig. 7. The time course of observed UGE was predicted dose-

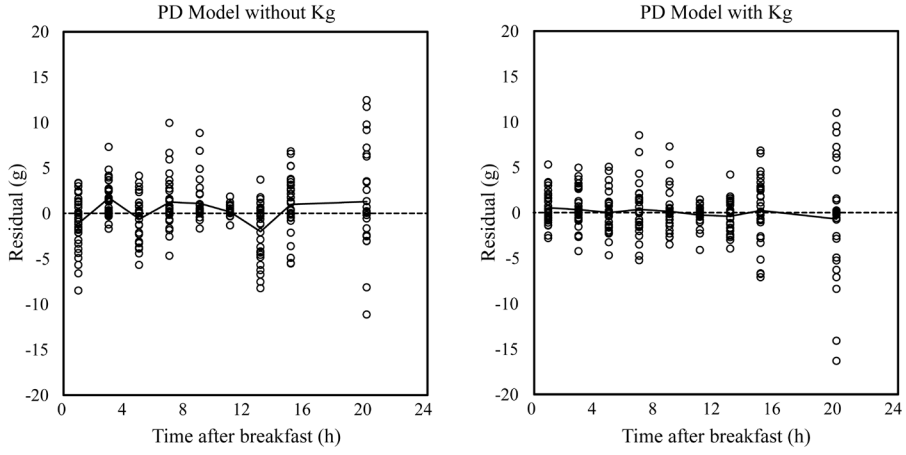


Fig. 4. Residuals against Time after Breakfast Started on Day −1 (Pharmacodynamic Models with $K_g$ and without $K_g$)

Dashed line, residual=0; Solid line, mean value of residuals; $K_g$, rate constant for excretion lag time; PD, pharmacodynamic.

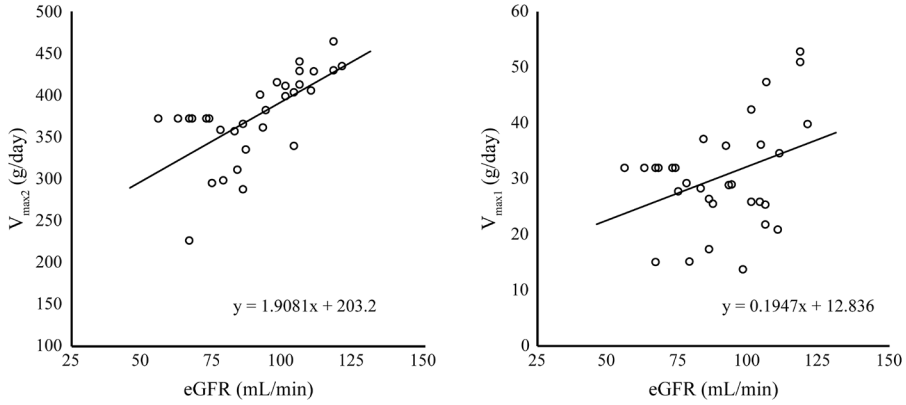


Fig. 5. Correlation between eGFR and $V_{max1}$ and $V_{max2}$

Solid line, predicted by linear regression; Open circles, individual $V_{max1}$ and $V_{max2}$ against eGFR; eGFR, estimated glomerular filtration rate; $V_{max1}$, transport capacity of SGLT1; $V_{max2}$, transport capacity of SGLT2; SGLT, sodium glucose co-transporter.

Table 4. Population Analysis of PK-PD Models

| PK-PD Model | Parameter estimate | | | | | | | | |
|---|---|---|---|---|---|---|---|---|---|
| | $K_{i2}$ nM | $K_{on}$ 1/nM/h | $K_{off}$ 1/h | $K_g$ 1/h | $T_{1/2,off}$ h | $\omega K_{i2}$ — | $\omega K_g$ — | Residual g | OBJ |
| Model 1 | 0.251 | — | — | 1.51 | — | 0.635 | — | 5.43 | 2961.685 |
| Model 2 | 0.336 | 0.303 | 0.102 | 2.20 | 6.81 | 0.527 | 0.0167 | 4.71 | 2785.244 |
| PK-PD Model | Parameter *in vitro* | | | | | Ratio *in vivo*/*in vitro* | | | |
| | $K_{i2}$ nM | $K_{on}$ 1/nM/h | $K_{off}$ 1/h | $K_g$ 1/h | $T_{1/2,off}$ h | $K_{i2}$ — | $K_{on}$ — | $K_{off}$ — | $T_{1/2,off}$ — |
| Model 1 | 1.10 | — | — | — | — | 0.23 | — | — | — |
| Model 2 | | 0.084 | 0.11 | — | 7.0 | 0.31 | 3.6 | 0.94 | 1.0 |

PK-PD model, pharmacokinetic-pharmacodynamic model; $K_{i2}$, inhibition constant of luseogliflozin to SGLT2; $K_{on}$, inhibition on rate of luseogliflozin to SGLT2; $K_{off}$, inhibition off rate of leusogliflozin from SGLT2 and luseogliflozin complex; $K_g$, rate constant for excretion lag time; $T_{1/2,off}$, half-time of $K_{off}$; $\omega K_{i2}$, interindividual variability of $K_{i2}$; $\omega K_{on}$, interindividual variability of $K_{on}$; OBJ, objective function of NONMEM; SGLT, sodium glucose co-transporter; Model 1, PK-PD model in which $K_{on}$ and $K_{off}$ are not considered for inhibition of SGLT2; Model 2, PK-PD model in which $K_{on}$ and $K_{off}$ are considered for inhibition of SGLT2; Parameter *in vitro*: ref 20.

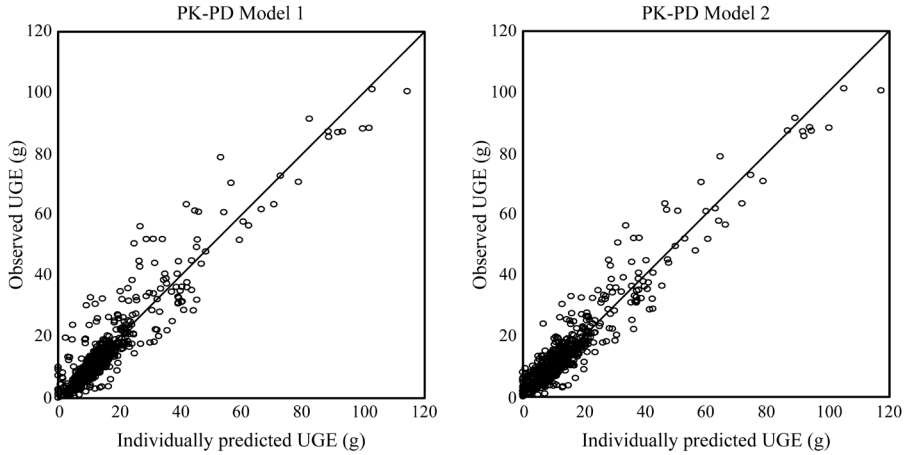


Fig. 6. Goodness-of-Fit Plots of Pharmacokinetic–Pharmacodynamic Models in Which $K_{on}$ and $K_{off}$ Are Considered (Model 2) and Not Considered (Model 1) for Inhibition of SGLT2

Solid line, observed UGE=individually predicted UGE; Open circles, plot of individual UGE; $K_{on}$, inhibition on rate; $K_{off}$, inhibition off rate; UGE, urinary glucose excretion; PK-PD, pharmacokinetic–pharmacodynamic; SGLT, sodium glucose co-transporter.

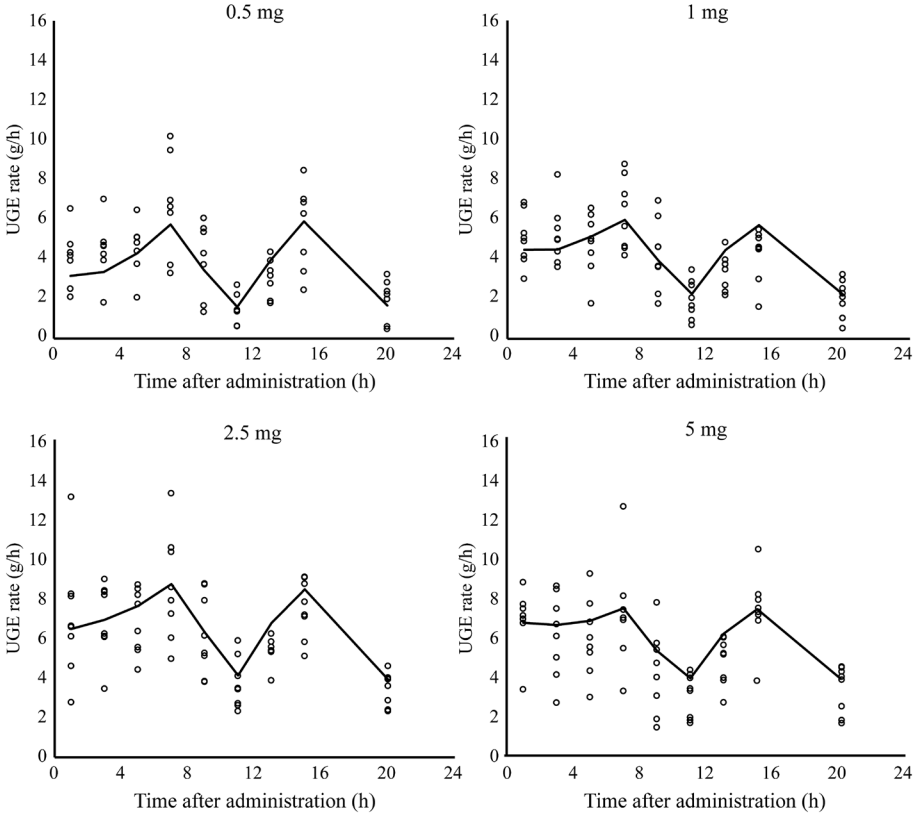


Fig. 7. Observed UGE and Mean Values of Individually Predicted UGE against Time on Selected Pharmacokinetic–Pharmacodynamic Model 2 by Dose on Day 7

Open circles, observed UGE rate; Line, mean values of individually predicted UGE; UGE, urinary glucose excretion.

dependently, and luseogliflozin's characteristic time course of UGE was also predicted.

Sensitivity Analysis of $K_{i1}$ and $K_1$

Estimated population mean, inter-individual variability, and residual UGE barely fluctuated with varying $K_{i1}$ values (195, 1950, and 19500 nM, respectively), and with varying $K_1$ values (0.3, 1, 3, and 10 l/(mg/mL)/h, respectively) in model 2. Accordingly, we concluded that model 2 was not sensitive for the values of $K_{i1}$ and $K_1$ in those ranges, and that the $K_{i1}$ value of 1950 nM and the $K_1$ value of 10 l/(mg/mL)/h used in the PK-PD model were reasonable for analysis.

The time course of the SGLT2 inhibition ratio for both PK-PD models is shown in Fig. 8. The time course of SGLT2 inhibition ratio in model 2 reflects the features of UGE.

**PK-PD Model Evaluation** A visual predictive check of UGE rates based on the PK-PD model (model 2) was performed. The time course of observed and predicted UGE rates for doses of 2.5 and 5 mg on day 7 is shown in Fig. 9. The 5, 50, and 95th percentiles of simulated UGE rates were reasonably comparable with the 50th percentiles and the 90%

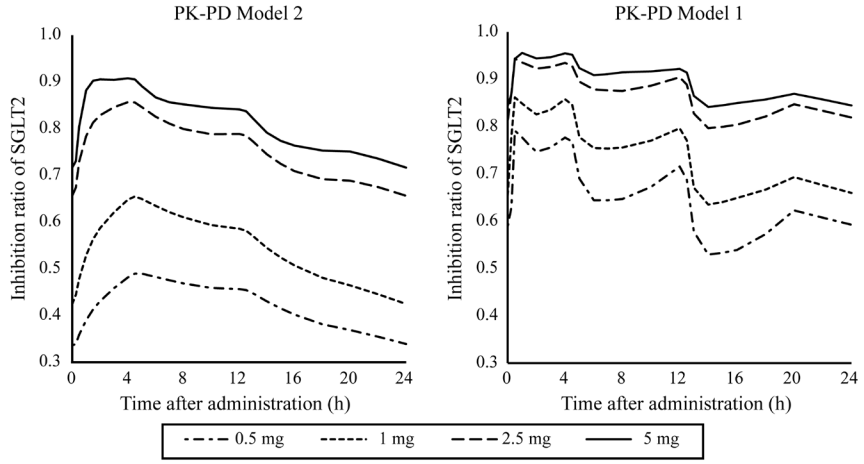


Fig. 8. Mean Predicted Inhibition Ratio of SGLT2 in Models 1 and 2 by Dose on Day 7

Lines, predicted mean inhibition ratio of SGLT2 for administration of 0.5–5 mg luseogliflozin on day 7; 0–4 h, time interval after breakfast; 4–8 h, time interval after lunch; 12–16 h, time interval after supper; PK-PD, pharmacokinetic–pharmacodynamic; SGLT, sodium glucose co-transporter.

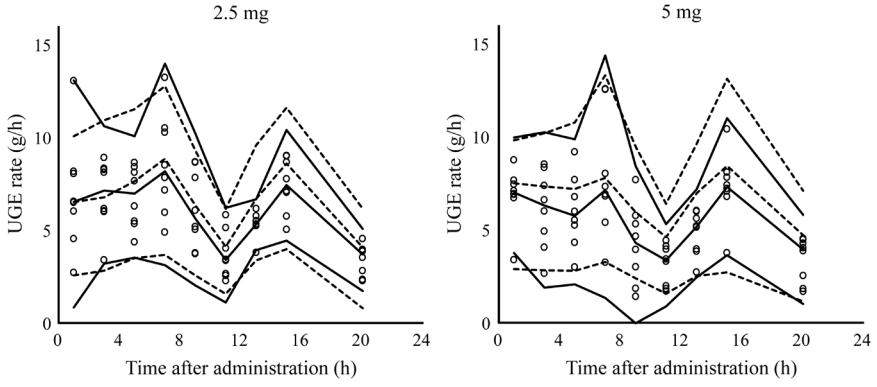


Fig. 9. Visual Predictive Check of UGE Rate on the Selected Pharmacokinetic–Pharmacodynamic Model in Which $K_{on}$ and $K_{off}$ Are Considered (Model 2), Administration of 2.5- and 5-mg Luseogliflozin, Day 7

Open circles, observed UGE rate; Solid line, 50th percentiles and 90% prediction intervals (central, bottom, and top) of observed UGE rate; Dashed lines, 5, 50, and 95th percentiles (from bottom to top) of simulated UGE rate; $K_{on}$, inhibition on rate; $K_{off}$, inhibition off rate; UGE, urinary glucose excretion.

prediction intervals of observed UGE rates, and most of the observed UGE rates were within the 90% interval of the simulated UGE rates. The predicted UGE rates generally described the characteristic time course of the observed UGE rates.

## DISCUSSION

The selected population PK-PD model 2 could describe the time course of the observed UGE after administration of luseogliflozin. We subsequently assessed the validity of the estimated value of the PD parameters and PK-PD parameter, $K_{i2}$, and considered the relevance of inhibition rate constants to sustained UGE.

**Validity of Estimated PD Parameters of $V_{max1}$, $V_{max2}$, and $K_g$** The mean (standard deviation (S.D.)) values of individually estimated $V_{max1}$ and $V_{max2}$ and contribution of $V_{max1}$ were 30 (10) and 376 (52) g/d, and 7% (2%), respectively. Because these are the first estimated values of $V_{max1}$ and $V_{max2}$ in Japanese patients with T2DM, we compared the values with other reports. Lu *et al*. reported a $V_{max1}$ of 86 g/d and $V_{max2}$ of 475 g/d for patients with T2DM.[18] The mean $V_{max1}$ and $V_{max2}$ in our study were less than those reported by Lu *et al*. The contribution of $V_{max1}$ was also less than that reported by Lu *et al*. As SGLT1 was thought to be responsible for 10% of glucose reabsorption, the $V_{max1}$ contribution of 7% was not an extremely low value.

The $V_{max}$ difference between these two reports might be attributable to not only race but also to eGFR values. Lu *et al.* reported eGFRs ranging from 109 to 127 mL/min for patients with T2DM. This was higher than for the Japanese patients in our study. Considering the relationship of $V_{max1}$ and $V_{max2}$ to eGFR, the $V_{max2}$ value of 376 g/d was adjusted to 411–446 g/d and the $V_{max1}$ value of 30 g/d was adjusted to 34–38 g/d. Though $V_{max1}$ was still lower, the $V_{max2}$ values of this report were then closer to the $V_{max2}$ of Lu *et al*. The reason for the relationship between $V_{max}$ and eGFR was unclear. However, hyperglycemia augments the expression and activity of SGLT2 in the renal proximal tubules,[1] and augmentation of eGFR is observed in patients with T2DM. A relationship between $V_{max}$ and eGFR is therefore possible. Accordingly, the $V_{max}$ values reported here are generally acceptable for Japanese patients with T2DM.

The rate constants for excretion lag time, $K_g$, were estimated to be 1.19 1/h without luseogliflozin administration and 2.20 1/h with luseogliflozin administration in model 2. These $K_g$ values indicate the remaining glucose that is absent from

SGLT reabsorption in the renal tubule takes a mean time of 0.84 or 0.45 h to appear in a urine sample. As the reversal of UGE in each meal interval against the *AUC* of plasma glucose was predicted by adopting $K_g$ to the PD model without luseogliflozin administration and the PK-PD model with luseogliflozin administration (Figs. 4, 7), we considered that a lag time existed between the UGE and plasma glucose peaks. Since, to our knowledge, there were no reports about measurement of the flow rate of luminal fluid and time required for the fluid to pass beyond the proximal tubule in humans, we could not determine the physiological validity of the $K_g$ value estimated from the PD and PK-PD models. We assumed that the lag time derives from the temporary retention of urine in the bladder. Urine remaining in the bladder is excreted in the next urine-collection interval, and the retention appears as lag time. As urine-collection intervals are two or eight hours, lag time of about one hour is possible.

The longer the lag time, the more UGE in the next urine-collection interval. The ratio of $(UGE_{2-4h})/(UGE_{0-2h})$ in each meal was 0.9–1.8, on day 7, but it was 0.9–3.0 on day −1 and that on day-1 was larger than on day 7 (Table 2), which was thought to be why the lag time of excretion without the inhibitor was longer than with the inhibitor.

**Validity of Estimated PK-PD Parameter of $K_{i2}$** As the mean prediction curve described the time course of observed UGE in all doses (Fig. 7), the estimated value of $K_{i2}$ on model 2 corresponded to the dose-dependency of luseogliflozin. However, the $K_{i2}$ value estimated on model 2 was one-third of the value *in vitro*; thus, to confirm the validity of $K_{i2}$ *in vivo*, we tried to calculate the $K_{i2}$ value from the $EC_{50}$ in a previous report.[9] Sasaki *et al.* calculated that $EC_{50}$, 254 ng·h/mL, by regression analysis of the $AUC_{0-24h}$ of plasma luseogliflozin concentration to the change in daily UGE from day −1. $EC_{50}$ could be converted to the mean free fraction of luseogliflozin over 24 h, 0.974 nM. This value was assumed to be the $IC_{50}$ of SGLT2, considering the low contribution of SGLT1. According to the relationship between inhibition constants ($K_i$) and $IC_{50}$,[31] $IC_{50}=K_i\times(1+Glu/K_m)$, $K_{i2}$ is calculated at 0.312 nM using the value of the $IC_{50}$, mean plasma glucose level over 24 h, (188 mg/dL), and $K_{m2}$. As the $K_{i2}$ value (0.312 nM), approximately calculated by the *E*max model of daily UGE, is nearly the same as the $K_{i2}$ value estimated by the PK-PD model (0.336 nM), we assumed it to be valid for the *in vivo* value.

Consequently, we examined the reason for the *in vivo* value being about one-third of the *in vitro* value. The low estimate of $K_{i2}$ *in vivo* compared with *in vitro* can be explained by the increased luminal luseogliflozin concentration. If luseogliflozin was secreted into the proximal tubule, the luminal luseogliflozin concentration could be increased. But renal clearance of free luseogliflozin is about 50 mL/min, less than the eGFR, and luseogliflozin is reabsorbed from the tubule. The luminal fluid is known to be condensed by almost three-fold when it reaches the end of the proximal tubule. But it is not obvious that luminal fluid is condensed three-fold at the site of SGLT2 in segment 1. As explained above, the difference between the $K_{i2}$ values *in vitro* and *in vivo* was not explained by secretion of luseogliflozin to the tubule or condensation of luminal fluid. Thus, we think that the difference was derived from experimentally using hSGLT2 expression cells *in vitro*, which is not the same circumstance as in the actual proximal tubule.

**Explanation of Sustained UGE over 24 h and Other Properties of UGE after Administration of Luseogliflozin** The dissociation half-time of luseogliflozin from SGLT2, calculated from the $K_{off}$ estimate based on model 2 was 6.81 h, and the dissociation delay was proven *in vivo* as well as *in vitro*. In Fig. 7, the mean prediction curve was fitted to the observed time course of UGE and the sustained UGE after supper appeared in the prediction curve. Accordingly, the assumption that sustained UGE results from the delay of dissociation of luseogliflozin from SGLT2 was thought to be correct.

Next, we considered the effect of another inhibition rate constant, $K_{on}$. As shown in Fig. 8, at all doses of luseogliflozin, the SGLT2 inhibition ratio in model 2 increased gradually, compared with plasma luseogliflozin up to 4 h, then decreased by 24 h. Because the $T_{max}$ of plasma luseogliflozin concentration was 1 h or less, the SGLT2 inhibition ratio peak was delayed after the plasma luseogliflozin peak. We thought the peak of the SGLT2 inhibition ratio indicated that the association of luseogliflozin to SGLT2 was delayed. In fact, the time course of the SGLT2 inhibition ratio was composed of both the association delay of $K_{on}$ and the dissociation delay of $K_{off}$. As shown in Table 5, sustained UGE after supper was accompanied by a UGE peak after lunch on day 7. The three time intervals in Fig. 8, 0–4, 4–8, and 12–16 h, represent each three-meal interval. The magnitude of the SGLT2 inhibition ratio of the three-meal interval in model 2 clearly illustrates the properties of UGE as described in Table 5. Temporary

Table 5. UGE Rate and Partial *AUC* of Plasma Glucose and Luseogliflozin on Day 7

| Variables | Time interval (after administration) | Unit | Dose | | | |
|---|---|---|---|---|---|---|
| | | | 0.5 mg | 1 mg | 2.5 mg | 5 mg |
| UGE rate | After breakfast (0–4 h) | (g/h) | 4.2 (1.4) | 5.1 (1.3) | 6.9 (2.3) | 6.5 (1.7) |
| | After lunch (4–8 h) | (g/h) | 5.5 (1.9) | 5.5 (1.0) | 7.7 (2.1) | 6.9 (2.6) |
| | After supper (12–16 h) | (g/h) | 4.2 (1.5) | 3.8 (0.9) | 6.4 (1.0) | 6.1 (1.4) |
| Partial *AUC* of plasma glucose | After breakfast (0–4 h) | (mg·h/dL) | 810 (156) | 780 (116) | 738 (102) | 708 (88) |
| | After lunch (4–8 h) | (mg·h/dL) | 887 (209) | 787 (126) | 802 (127) | 710 (105) |
| | After supper (12–16 h) | (mg·h/dL) | 924 (108) | 824 (125) | 828 (63) | 755 (137) |
| Partial *AUC* of luseogliflozin | After breakfast (0–4 h) | (ng·h/mL) | 58 (9) | 124 (21) | 289 (67) | 644 (83) |
| | After lunch (4–8 h) | (ng·h/mL) | 39 (7) | 80 (12) | 200 (33) | 411 (82) |
| | After supper (12–16 h) | (ng·h/mL) | 22 (5) | 46 (8) | 113 (22) | 230 (42) |

Values are mean (S.D.). *AUC*, area under the curve; UGE, urinary glucose excretion.

rises, which depend on low glucose levels, were observed at 4 and 12 h in the inhibition ratio of SGLT2 in model 1, but the inhibition ratio decreased more steadily and uniformly in this model. Because it is difficult for model 1 to describe the time course of UGE that conflicts with the concentration of the inhibitor, the good fit with model 2 was thought to derive from both inhibition rate constants in that model.

Based on these explanations, by adopting the inhibition rate constants to a competitive inhibition model, the PK-PD model could address the delay of association and dissociation of luseogliflozin, and could explain the delay of the UGE peak and the sustained UGE after administration of luseogliflozin. Moreover, since UGE was sustained up to 24 h, and consequently, lowering of plasma glucose was maintained after supper with once-daily dosage in the morning,[9] it became clear that these results derived from the kinetic characteristics of lower $K_{on}$ and $K_{off}$.

## CONCLUSION

To elucidate the effect of the inhibition rate constants, $K_{on}$ and $K_{off}$, and to explain the sustained UGE, the mechanism-based PK-PD model was constructed based on the action of glucose filtration in the glomerulus and reabsorption in the proximal tubule of the kidney, as well as on the kinetics of competitive inhibition of SGLTs and the inhibition rate constant for SGLT2 by using UGE, plasma glucose levels, and luseogliflozin concentrations in Japanese patients with T2DM. The acquired population PK-PD model fit the actual UGE, and the estimated population $K_{i2}$, $K_{on}$, and $K_{off}$ were within 0.31- to 3.6-fold of the corresponding *in vitro* values. Dissociation half-life of luseogliflozin from SGLT2, calculated from $K_{off}$, 6.81 h, was consistent with the value *in vitro*; therefore, the assumption that the sustained UGE was explained by the dissociation half-time was deemed correct. The inhibition ratio of SGLT2 on day 7, calculated on the acquired model, showed the delay of association of luseogliflozin to SGLT2, the peak at about 4 h after administration, and the same level at 24 h as just after administration. This model can explain luseogliflozin's UGE time course, *i.e.*, the UGE peak occurs after lunch and the UGE after supper is as same as after breakfast. Because the inhibition ratio of SGLT2, calculated on the model without inhibition rate constants, decreased along with the plasma concentration of luseogliflozin, the introduction of both inhibition rate constants to the PK-PD model was necessary for predicting UGE after luseogliflozin administration. Consequently, the small $K_{on}$ and $K_{off}$ were thought to generate the usefulness of luseogliflozin due to sustained UGE 24 h after administration and decreased plasma glucose maintained after supper when the drug was dosed once daily in the morning.

**Acknowledgments** The authors thank Dr. Teisuke Takahashi and Dr. Saeko Uchida for advice regarding kinetics of SGLT2 inhibition, Dr. Yasuhiro Nakai, Dr. Atsushi Furuya, Dr. Yukihiro Chino, and Ms. Yoko Mano for valuable inputs during the preparation of this manuscript, and Cactus Communications Pvt. Ltd. for editorial assistance.

**Conflict of Interest** All the authors are employees of Taisho Pharmaceutical Co., Ltd. This study was funded by Taisho Pharmaceuticals.

**Supplementary Material** The online version of this article contains supplementary materials.

## REFERENCES

1) DeFronzo RA, Davidson JA, Del Prato S. The role of the kidneys in glucose homeostasis: a new path towards normalizing glycaemia. *Diabetes Obes. Metab.*, **14**, 5–14 (2012).
2) Sha S, Devineni D, Ghosh A, Polidori D, Chien S, Wexler D, Shalayda K, Demarest K, Rothenberg P. Canagliflozin, a novel inhibitor of sodium glucose co-transporter 2, dose dependently reduces calculated renal threshold for glucose excretion and increases urinary glucose excretion in healthy subjects. *Diabetes Obes. Metab.*, **13**, 669–672 (2011).
3) Kasichayanula S, Chang M, Hasegawa M, Liu X, Yamahira N, LaCreta FP, Imai Y, Boulton DW. Pharmacokinetics and pharmacodynamics of dapagliflozin, a novel selective inhibitor of sodium–glucose co-transporter type 2, in Japanese subjects without and with type 2 diabetes mellitus. *Diabetes Obes. Metab.*, **13**, 357–365 (2011).
4) Scheen AJ. Pharmacokinetic and pharmacodynamic profile of empagliflozin, a sodium glucose co-transporter 2 inhibitor. *Clin. Pharmacokinet.*, **53**, 213–225 (2014).
5) Kakinuma H, Oi T, Hashimoto-Tsuchiya Y, Arai M, Kawakita Y, Fukasawa Y, Iida I, Hagima N, Takeuchi H, Chino Y, Asami J, Okumura-Kitajima L, Io F, Yamamoto D, Miyata N, Takahashi T, Uchida S, Yamamoto K. (1*S*)-1,5-Anhydro-1-[5-(4-ethoxybenzyl)-2-methoxy-4-methylphenyl]-1-thio-D-glucitol (TS-071) is a potent, selective sodium–dependent glucose cotransporter 2 (SGLT2) inhibitor for type 2 diabetes treatment. *J. Med. Chem.*, **53**, 3247–3261 (2010).
6) Yamamoto K, Uchida S, Kitano K, Fukuhara N, Okumura-Kitajima L, Gunji E, Kozakai A, Tomoike H, Kojima N, Asami J, Toyoda H, Arai M, Takahashi T, Takahashi K. TS-071 is a novel, potent and selective renal sodium–glucose cotransporter 2 (SGLT2) inhibitor with anti-hyperglycaemic activity. *Br. J. Pharmacol.*, **164**, 181–191 (2011).
7) Sasaki T, Seino Y, Fukatsu A, Sakai S, Samukawa Y. Safety, pharmacokinetics, and pharmacodynamics of single and multiple luseogliflozin dosing in healthy Japanese males: a randomized, single-blind, placebo-controlled trial. *Adv. Ther.*, **31**, 345–361 (2014).
8) Seino Y, Sasaki T, Fukatsu A, Sakai S, Samukawa Y. Efficacy and safety of luseogliflozin monotherapy in Japanese patients with type 2 diabetes mellitus: a 12-week, randomized, placebo-controlled, phase II study. *Curr. Med. Res. Opin.*, **30**, 1219–1230 (2014).
9) Sasaki T, Seino Y, Fukatsu A, Ubukata M, Sakai S, Samukawa Y. Pharmacokinetics, pharmacodynamics, and safety of luseogliflozin in Japanese patients with type 2 diabetes mellitus: a randomized, single-blind, placebo-controlled trial. *Adv. Ther.*, **32**, 319–340 (2015).
10) Seino Y, Sasaki T, Fukatsu A, Ubukata M, Sakai S, Samukawa Y. Dose-finding study of luseogliflozin in Japanese patients with type 2 diabetes mellitus: a 12-week, randomized, double-blind, placebo-controlled, phase II study. *Curr. Med. Res. Opin.*, **30**, 1231–1244 (2014).
11) Seino Y, Sasaki T, Fukatsu A, Ubukata M, Sakai S, Samukawa Y. Efficacy and safety of luseogliflozin as monotherapy in Japanese patients with type 2 diabetes mellitus: a randomized, double-blind, placebo-controlled, phase 3 study. *Curr. Med. Res. Opin.*, **30**, 1245–1255 (2014).
12) Seino Y, Inagaki N, Haneda M, Kaku K, Sasaki T, Fukatsu A, Ubukata M, Sakai S, Samukawa Y. Efficacy and safety of luseogliflozin added to various oral antidiabetic drugs in Japanese patients with type 2 diabetes mellitus. *J. Diabetes Investig.*, **6**, 443–453 (2015).
13) Maurer TS, Ghosh A, Haddish-Berhane N, Sawant-Basak A, Boustany-Kari CM, She L, Leininger MT, Zhu T, Tugnait M, Yang

X, Kimoto E, Mascitti V, Robinson RP. Pharmacodynamic model of sodium–glucose transporter 2 (SGLT2) inhibition: implications for quantitative translational pharmacology. *AAPS J.*, **13**, 576–584 (2011).
14) Devineni D, Curtin CR, Polidori D, Gutierrez MJ, Murphy J, Rusch S, Rothenberg PL. Pharmacokinetics and pharmacodynamics of canagliflozin, a sodium glucose co-transporter 2 inhibitor, in subjects with type 2 diabetes mellitus. *J. Clin. Pharmacol.*, **53**, 601–610 (2013).
15) Mondick J, Riggs M, Sasaki T, Sarashina A, Broedl UC, Retlich S. Mixed-effects modelling to quantify the effect of empagliflozin on renal glucose reabsorption in patients with type 2 diabetes. *Diabetes Obes. Metab.*, **18**, 241–248 (2016).
16) Yamaguchi K, Kato M, Suzuki M, Asanuma K, Aso Y, Ikeda S, Ishigai M. Pharmacokinetic and pharmacodynamic modeling of the effect of an sodium–glucose cotransporter inhibitor, phlorizin, on renal glucose transport in rats. *Drug Metab. Dispos.*, **39**, 1801–1807 (2011).
17) Yamaguchi K, Kato M, Suzuki M, Hagita H, Takada M, Ayabe M, Aso Y, Ishigai M, Ikeda S. *In vitro–in vivo* correlation of the inhibition potency of sodium–glucose cotransporter inhibitors in rat: a pharmacokinetic and pharmacodynamic modeling approach. *J. Pharmacol. Exp. Ther.*, **345**, 52–61 (2013).
18) Lu Y, Griffen SC, Boulton DW, Leil TA. Use of systems pharmacology modeling to elucidate the operating characteristics of SGLT1 and SGLT2 in renal glucose reabsorption in humans. *Front. Pharmacol.*, **5**, 274 (2014).
19) Mori K, Saito R, Nakamaru Y, Shimizu M, Yamazaki H. Physiologically based pharmacokinetic–pharmacodynamic modeling to predict concentrations and actions of sodium–dependent glucose transporter 2 inhibitor canagliflozin in human intestines and renal tubules. *Biopharm. Drug Dispos.*, **37**, 491–506 (2016).
20) Uchida S, Mitani A, Gunji E, Takahashi T, Yamamoto K. *In vitro* characterization of luseogliflozin, a potent and competitive sodium glucose co-transporter 2 inhibitor: inhibition kinetics and binding studies. *J. Pharmacol. Sci.*, **128**, 54–57 (2015).
21) Tamura Y, Miyagawa H, Yoshida T, Chuman H. Binding interaction of SGLT with sugar and thiosugar by the molecular dynamics simulation. *Biochim. Biophys. Acta*, **1848** (11 Pt A), 2799–2804 (2015).
22) Imai E, Yasuda Y, Makino H. Japan Association of Chronic Kidney Disease Initiatives (J-CKDI). *J.M.A.J.*, **54**, 403–405 (2011).
23) Segel IH. *Enzyme Kinetics: Behavior and Analysis of Rapid Equilibrium and Steady-state Enzyme Systems*. Wiley Interscience, New York, chapter 3 (1993).
24) Dahl G, Akerud T. Pharmacokinetics and the drug-target residence time concept. *Drug Discov. Today*, **18**, 697–707 (2013).
25) Hummel CS, Lu C, Liu J, Ghezzi C, Hirayama BA, Loo DD, Kepe V, Barrio JR, Wright EM. Structural selectivity of human SGLT inhibitors. *Am. J. Physiol. Cell Physiol.*, **302**, C373–C382 (2012).
26) Cer RZ, Mudunuri U, Stephens R, Lebeda FJ. $IC_{50}$-to-$K_i$: a web-based tool for converting $IC_{50}$ to $K_i$ values for inhibitors of enzyme activity and ligand binding. *Nucleic Acids Res.*, **37** (Web Server), W441–W445 (2009).
27) Hasegawa M, Chino Y, Horiuchi N, Hachiuma K, Ishida M, Fukasawa Y, Nakai Y, Yamaguchi J. Preclinical metabolism and disposition of luseogliflozin, a novel antihyperglycemic agent. *Xenobiotica*, **45**, 1105–1115 (2015).
28) Hummel CS, Lu C, Loo DDF, Hirayama BA, Voss AA, Wright EM. Glucose transport by human renal Na+/d-glucose cotransporters SGLT1 and SGLT2. *Am. J. Physiol. Cell Physiol.*, **300**, C14–C21 (2011).
29) Segel IH. *Enzyme Kinetics: Behavior and Analysis of Rapid Equilibrium and Steady-state Enzyme Systems*. Wiley Interscience, New York, chapter 1 (1993).
30) Karlsson MO, Holford N. "A tutorial on visual predictive checks." PAGE 17, Abstr 1434. (2008).: ‹www.page-meeting.org/?abstract=1434›, cited 26 June 2017.
31) Cortés A, Cascante M, Cardenas M, Cornish-Bowden A. Relationships between inhibition constants, inhibitor concentrations for 50% inhibition and types of inhibition: new ways of analysing data. *Biochem. J.*, **357**, 263–268 (2001).